Journal of Materials Chemistry A

PAPER

View Article Online
View Journal | View Issue

Cite this: J. Mater. Chem. A, 2019, 7, 4823

Length evolution of fused-ring electron acceptors toward optimal blend morphology in polymer solar cells incorporating asymmetric benzodithiophene-based donors†

Qianqian Zhu,‡[a] Deyu Liu,‡[bc] Zhou Lu,[a] Chunyang Gu,[b] Kaili Zhang,[b] Xichang Bao, *[b] Qun Li[a] and Renqiang Yang *[b]

Two new wide-bandgap polymers (PBDTBDD-Ph and PBDTBDD-PhPh) with different aggregation degrees and fused-ring electron acceptors (FREAs) (ITIC-4T, ITIC-3T and ITIC-2T) with different sizes were synthesized. The work was used to understand how to design the donor polymers and fused-ring electron acceptors (FREAs) for high-performance non-fullerene polymer solar cells (NF-PSCs). The results clearly demonstrated that weakly aggregated donor polymers and small-sized FREAs in appropriate degrees can match well with each other to achieve high power conversion efficiencies (PCEs). In other words, small-sized FREAs can be embedded more easily into the interspace of polymer chains and weakly aggregated polymers can offer larger space for the intercalation of FREAs. As a result, an NF-PSC device based on weakly aggregated polymer PBDTBDD-Ph and small-sized ITIC-3T yielded over 11% PCE. Thus, it would offer a feasible guideline to design high-performance NF-PSCs that meet the requirement of future industry-scale production.

Received 26th November 2018
Accepted 29th January 2019

DOI: 10.1039/c8ta11363g

rsc.li/materials-a

Introduction

Polymer solar cells (PSCs) have attracted signi珡cant attention from academics and industry because of their advantages of light weight, mechanical 珠exibility and potentially large areas.[1–7] The most efficient PSCs are fabricated using a bulk heterojunction (BHJ) structure with a p-type conjugated polymer as the donor and an n-type semiconductor as the acceptor. In the past few years, bene珡ting from the rapid development of fused-ring electron acceptors (FREAs) due to their better absorption in the visible spectral region and more facile energy-level modulation, non-fullerene polymer solar cells (NF-PSCs) have made signi珡cant progress.[8–18] Some FREA systems have boosted the power conversion efficiencies (PCEs) of NF-PSCs over 14%.[19,20]

Typically, the reported efficient FREAs have acceptor–donor–acceptor (A–D–A)-type structural characteristics.[21–23] In this type of structure, planar aromatic fused rings, such as indacenodithieno[3,2-*b*]thiophene (IDTT),[22] are used as the donor core, and electron-withdrawing units, such as 3-(dicyanomethylidene)indan-1-one (IC),[22] serve as the acceptor terminal. Compared to traditional fullerene acceptors, such as phenyl-C_{61}-butyric acid methyl ester ($PC_{61}BM$) and phenyl-C_{71}-butyric acid methyl ester ($PC_{71}BM$), FREAs present their impressive advantages as follows. (1) Stronger absorption in the visible and even near infrared region can be obtained by using excellent central fused rings and acceptor terminals. As a result, more photons can be captured and the short-circuit current density (J_{SC}) is improved.[24,25] (2) By changing the end-capping electron-de珡cient groups of the acceptor, the appropriate frontier molecular orbital levels of the acceptor can combine well with those of the donor polymers and guarantee high open circuit voltage (V_{OC}).[26,27] Although these two advantages of FREAs have been proven to increase PCEs of PSCs, the elongated plane in their geometry makes it difficult to control the morphology of the active layer.[28] Thus, the morphologies of the active layers in almost all high-performance NF-PSCs need to be optimized using additional complicated treatments such as solvent additive processing and thermal/solvent annealing.[12,29–31] These complicated treatments go against the simple, low-cost industry-scale production of large-area solar cells.

To overcome this problem, recently, we proposed an efficient strategy from the viewpoint of molecular structure to design donor polymers that can generate preferred morphologies of active layers, which can then be used to fabricate high-

[a]College of Chemistry and Chemical Engineering, Qingdao University, Qingdao 266071, China

[b]CAS Key Laboratory of Bio-based Materials, Qingdao Institute of Bioenergy and Bioprocess Technology, Chinese Academy of Sciences, Qingdao 266101, China. E-mail: yangrq@qibebt.ac.cn; baoxc@qibebt.ac.cn

[c]University of Chinese Academy of Sciences, Beijing 100049, China

†Electronic supplementary information (ESI) available. See DOI: 10.1039/c8ta11363g

‡ Qianqian Zhu and Deyu Liu contributed equally to this work.

performance NF-PSCs without post-treatments.[32] The new two-dimensional (2D) asymmetric benzodithiophene (BDT) building blocks were employed to construct the polymers. In these structures, the thienylthiol group with a long alkyl chain as one side chain on the BDT unit could modulate energy levels, broaden absorption spectra and improve solubility. For another side chain, the bare rigid aryl rings could be regarded as lever arms to stir up the elongated non-fullerene acceptor well in the solution of the blends and weaken the entanglements among polymer chains during the spin-coating process, which enabled favorable morphology without post-treatments. Compared to conventional symmetric BDT units, the key feature of a 2D asymmetric structure is that it can efficiently control the morphology of the blend 莽lm with the elongated nonfullerene acceptor and simplify device fabrication. Although some insights are given into controlling the morphologies of NF-PSCs from the donor polymer point of view, there is almost no guideline currently available for a non-fullerene acceptor itself.

In 2015, Zhan *et al.* reported original FREA with an A–D–A structure exempli莽ed by ITIC[22] (namely, ITIC-4T, Fig. 1). Since then, a series of ITIC derivatives, such as ITIC1,[33] ITIC2 (ref. 33) and ITIC-Th,[34] have been reported in the NF-PSC 莽eld. Based on the system, many donor polymers achieved very high PCEs. Thus, in this manuscript, we selected ITIC for the study of blend morphology. It is noteworthy that $PC_{71}BM$ and ITIC with almost same carbon atomic numbers showed signi莽cant difference in geometries. $PC_{71}BM$ is roughly spherical with a small number of solubilizing groups, while ITIC is elongated plane-shaped with signi莽cantly more solubilizing groups. This resulted in different morphologies of active layers. As reported in our previous studies,[28,32] unlike spherical $PC_{71}BM$, elongated ITIC can only be embedded well into sufficient interspace among the weakly aggregated polymer chains, which forms a favorable micro-structure. Thus, decreasing the length of ITIC will be one key for favorable morphology and high-performance NF-PSCs.

In this regard, we decreased the length of ITIC *via* cutting one thiophene ring of the fused-ring backbone and synthesized the acceptor ITIC-3T (Fig. 1). In fact, there is another location to decrease the size: the side chains (four rigid phenyl side chains). However, their functions for improving solubility and restricting severe self-aggregation could not be replaced. For comparison, we synthesized other two acceptors, as reported in literatures: longer ITIC-4T[22] and shorter ITIC-2T (namely, IC-1IDT-IC),[35] as shown in Fig. 1. By studying the three molecules, we investigated the effects of the lengths of backbones on the morphologies of active layers. Furthermore, we still adopted promising asymmetric BDT building blocks and employed two types of rigid aryl rings (benzene and biphenyl) as one side chain to construct the donor polymers with different degrees of self-aggregations. Based on the well-known acceptor unit 1,3-bis(5-bromothiophen-2-yl)-5,7-bis(2-ethylhexyl)-4*H*,8*H*-benzo[1,2-*c*:4,5-*c*′]dithiophene-4,8-dione (BDD), two new wide-bandgap polymers (PBDTBDD-Ph and PBDTBDD-PhPh) were synthesized, as shown in Fig. 1. In addition, the polymer PBDTsTh-BDD[28] (Fig. 1) with stronger self-aggregation reported previously by us was chosen as a contrast. Three polymers were applied to three FREAs (ITIC-4H, ITIC-3H and ITIC-2H). As a result, it was found that decreasing the size of FREAs adequately was efficient for improving photovoltaic properties. Compared to classic ITIC-4T-based devices, ITIC-3T-based devices showed higher PCEs. In particular, the PBDTBDD-Ph:ITIC-3T solar cells achieved impressive PCE of 11.02%. It is unreasonable to decrease the size of FREAs to a large extent. These devices based on ITIC-2T with minimum sizes showed the worst photovoltaic performance with PCEs less than 7%. Meanwhile, the devices based on PBDTBDD-Ph achieved higher PCEs than those based on PBDTsTh-BDD and PBDTBDD-PhPh. The results further con莽rmed our viewpoint in our previous report[28] that decreasing the self-aggregation of donor polymers adequately was bene莽cial for blending with FREAs for high efficiencies.

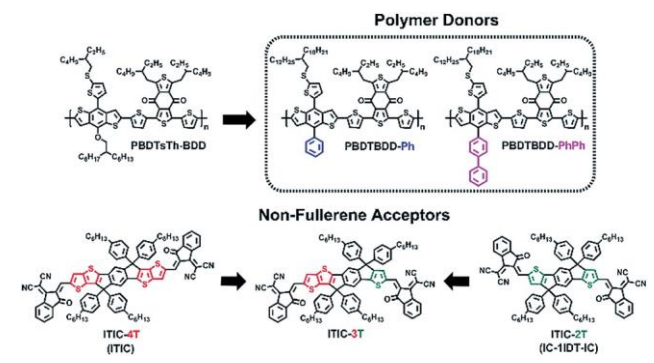

Fig. 1 Chemical structures of materials used in PSCs.

Results and discussion

The synthetic routes of donor polymers and non-fullerene acceptors are outlined in Scheme S1,† and the synthetic procedures are described in the ESI.† The polymers were obtained through Stille polymerization using $Pd(PPh_3)_4$ as the catalyst. The synthesized polymers and acceptor could be dissolved in common solvents such as chloroform, chlorobenzene (CB) and *o*-dichlorobenzene (DCB). The number-average molecular weight (M_n) and polydispersity index (PDI) were measured by gel permeation chromatography (GPC) using THF as the eluant and polystyrene as the internal standard. The M_n values of PBDTBDD-Ph and PBDTBDD-PhPh were 48.6 and 55.8 KDa, respectively (Table S1†). The thermal properties of the materials were determined by thermogravimetric analysis (TGA), as shown in Fig. S1.† The TGA results revealed that the onset temperature with 5% weight loss (T_d) of all materials was over 300 °C (Table S1†). These values indicated that the thermal stability of the materials is good enough for NF-PSC applications.

Density functional theory (DFT) calculations using the Gaussian 09 program at the B3LYP/6-31G(d,p) level[36] were performed to gain insights into the chemical geometries of FREAs and polymers with simpli莽ed side chains. As shown in Fig. 2, three FREAs (ITIC-4T, ITIC-3T and ITIC-2T) exhibit similar 莽at backbone con莽gurations *via* S⋯O noncovalent interactions, while hexylphenyl substituents on the donor cores exhibit large

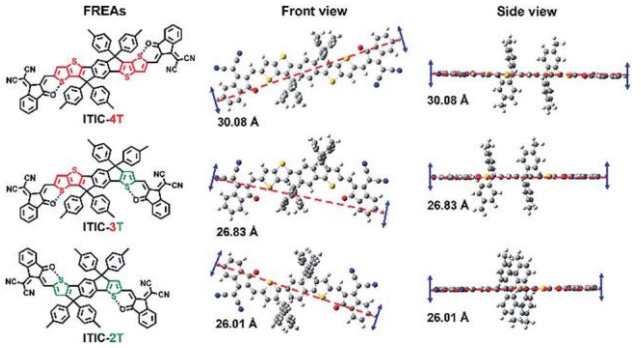

Fig. 2 Simulated molecular geometries and calculated molecular sizes of FREAs by DFT calculations.

twisted angles to the backbone plane. In addition, we calculated and then compared the length evolution. As clearly demonstrated in Fig. 2, the lengths of the molecules shortened as the number of the fused rings in the backbone decreased. Please note that the length of ITIC-3T was 26.83 Å; it was much shorter than that of ITIC-4T and slightly longer than that of ITIC-2T. As we expected, cutting one thiophene ring of the fused-ring backbone could shorten the size of the molecules efficiently while maintaining sufficient conjugated degree. As shown in Fig. S2,† two new polymers (PBDTBDD-Ph and PBDTBDD-PhPh) exhibit large dihedral angles (from 56° to 59°) between the aryl side chains and BDT backbones, which can weaken polymeric self-aggregation and offer some space for acceptors. Especially, the extra benzene ring of PBDTTAZ-PhPh resulted in almost vertical twisting with the polymer backbone, further weakening the polymeric self-packing.

The UV-vis absorption spectra of donor polymers and acceptors in thin 珋lms and in chlorobenzene solutions at room temperature are shown in Fig. 3a and S3a,† respectively, and the corresponding absorption properties are summarized in Table S1.† As shown in Fig. 3a, the absorption edges (l_{onset}) of ITIC-4T, ITIC-3T and ITIC-2T are 785, 769 and 738 nm, respectively, and their E_g^{opt} values are estimated to be 1.58, 1.61 and 1.68 eV, respectively, according to E_g^{opt} ¼ 1240/l_{onset} from the l_{onset} values of 珋lm absorption. Compared to ITIC-4T, ITIC-2T exhibited signi珋cant blue-shi沢 (rv27 nm) in the major absorption, which is not bene珋cial to capture photons. However, ITIC-3T with one thiophene ring cleaved from the fused-ring backbone showed slight blue-shi沢 (rv5 nm), which guaranteed the absorption of photons for excellent J_{SC}. Two wide-bandgap polymers displayed similar hump-shaped absorption pro珋les.

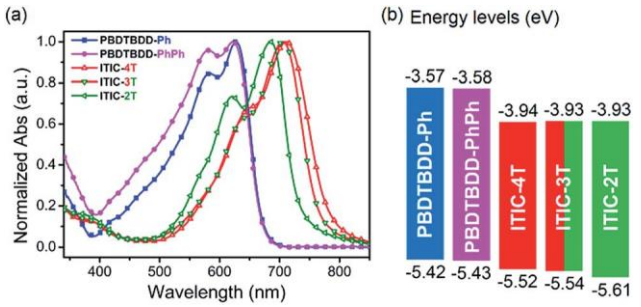

Fig. 3 (a) Absorption spectra of donors and acceptors in the solid state. (b) Energy level diagrams of donors and acceptors.

The E_g^{opt} values of PBDTBDD-Ph and PBDTBDD-PhPh were estimated to be the same (1.85 eV). From the UV-vis absorption results, we inferred that the two polymers exhibited complementary absorption with ITIC-4T and ITIC-3T.

The electrochemical properties of donor polymers and acceptors were investigated by electrochemical cyclic voltammetry (CV).[37] The CV curves are shown in Fig. S3† and the results of electrochemical properties are listed in Table S1.† The energy levels of donor polymers and acceptors used for solar cell devices are also shown in Fig. 3b. The HOMO energy levels of the two polymers were deep-lying, which is bene珋cial for V_{OC}. For three acceptors, the HOMO energy level of ITIC-3T with cutting one thiophene ring of the fused-ring backbone was slightly deeper than that of ITIC-4T. Upon cutting two thiophene rings, ITIC-2T showed a much deeper HOMO energy level (—5.61 eV). The LUMO energy levels of the polymers were higher-lying than those of acceptors, which could form energy cascade and favor electron transfer.

Photovoltaic properties of the polymers and acceptors were investigated with a conventional con珋guration of ITO/PEDOT:PSS/active layer materials/PFN-Br/Al. Current density *versus* voltage (*J*–*V*) curves and the corresponding data of the optimized devices under illumination of AM 1.5G (100 mW cm^{-2}) are shown in Fig. 4a–c and Table 1, respectively. Different D/A ratios, thermal annealing and additive processing (1,8-diiodooctane, DIO) were used to optimize the photovoltaic performance; the corresponding data are shown in Tables S2–S4.† The strongly aggregated polymer PBDTsTh-BDD showed improved photovoltaic performance after blending with small sized ITIC-3T. PCE increased from 7% to 9% compared with that of the ITIC-4T system. For the weakly aggregated polymer PBDTBDD-Ph, there was adequate space for ITIC-3T to be well embedded. As a result, the PBDTBDD-Ph:ITIC-3T solar cells produced remarkable PCE of 11.02% with V_{OC} of 0.924 V, J_{SC} of 17.51 mA cm^{-2}, and FF of 0.681. After blending with longer sized ITIC-4T, the PBDTBDD-Ph-based device showed lower PCE of 9.90%. Upon further weakening the self-aggregation of polymer by introducing biphenyl groups as side chains, PBDTBDD-PhPh-based devices showed much lower PCEs. This was attributed to the poor morphologies caused by excessive destruction of polymer chain packing. In addition, it is worth noting that the three devices based on ITIC-2T with minimum sizes did not show improved photovoltaic performances with PCEs less than 7% compared with ITIC-4T- and ITIC-3T-based solar cells. This was mainly due to much narrower absorption spectra, which caused lower J_{SC} values. Therefore, self-aggregation of donor polymers and size of acceptors are the two key factors for achieving highly efficient PSCs.

The corresponding external quantum efficiencies (EQEs) of the devices were measured; (Fig. 4d–f). ITIC-4T, ITIC-3T and ITIC-2T-based blends exhibited different absorptions in the ranges of 340–800 nm, 340–780 nm and 340–740 nm, respectively. Especially, the EQE value of PBDTBDD-Ph:ITIC-3T was

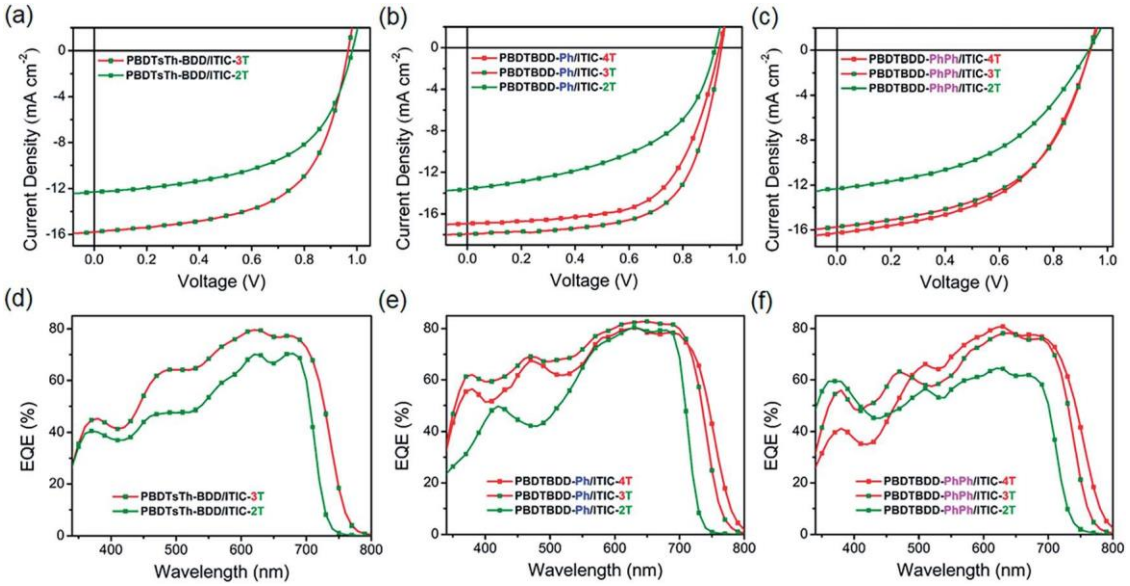

Fig. 4 *J*–*V* curves for the optimized devices under the illumination of AM 1.5G (100 mW cm^{-2}): (a) PBDTsTh-BDD/different acceptor-based devices; (b) PBDTBDD-Ph/different acceptor-based devices; (c) PBDTBDD-PhPh/different acceptor-based devices. EQE curves for the optimized devices under the illumination of AM 1.5G (100 mW cm^{-2}): (d) PBDTsTh-BDD/different acceptor-based devices; (e) PBDTBDD-Ph/different acceptor-based devices; (f) PBDTBDD-PhPh/different acceptor-based devices.

very high in the whole spectra and the maximum value reached 82%, indicating that the device exhibited better photoresponse among the absorption ranges. For ITIC-2T-based blends, three EQE curves exhibit the weakest photoresponse in the range of 340–740 nm. Therefore, the devices yielded much lower J_{SC}. The calculated current densities from the EQE measurements are summarized in Table 1, which agree well with J_{SC} obtained from the *J*–*V* measurements.

Charge carrier mobility is another important factor that influences device performance. The hole and electron mobilities (m_h and m_e) were measured *via* the space charge limited current (SCLC)[38] method (Fig. S4 and S5†). The calculated m_h and m_e values are listed in Table S5.† Compared with PBDTsTh-BDD/ITIC[28] and PBDTBDD-PhPh/ITIC blends, the PBDTBDD-Ph/ITIC blend exhibited higher m_h. For the PBDTBDD-Ph system, the ITIC-3T-based device showed much higher m_h than ITIC-4T and ITIC-2T-based devices, which was beneficial for higher J_{SC}. In addition, balanced carrier transport in active layers is quite important and can lead to high FF. Therefore, PBDTBDD-Ph/ITIC-3T-based devices gave the highest FF (0.681) probably due to the excellent balanced carrier transport (m_e/m_h ¼ 1.71). The ITIC-2T-based device showed unbalanced carrier transport, which could result in poor FF.

Photoluminescence (PL) was also measured to investigate energy transfer and exciton dissociation process in PBDTBDD-Ph/ITIC-4T, PBDTBDD-Ph/ITIC-3T and PBDTBDD-Ph/ITIC-2T blend films, as shown in Fig. S6.† A pure PBDTBDD-Ph film exhibited strong PL around 660 nm, and the PL emission of blend films was markedly quenched, indicating that there existed some PL quenching channels for charge transfer between PBDTBDD-Ph and small-sized acceptors in blend films. Photo-generated excitons were dissociated before luminescence occurred. Notably, PL intensities of PBDTBDD-Ph/ITIC-4T and PBDTBDD-Ph/ITIC-3T were significantly suppressed; this

Table 1 Photovoltaic properties of the polymers and acceptors

Polymers	Acceptors	D/A (w/w)	Thermal annealing[a] (°C)	V_{OC} (V)	J_{SC}[b] (mA cm^{-2})	FF	PCE[c] (%)	Ref.
PBDTsTh-BDD	ITIC-4T	1 : 1	100	0.954	14.02 (13.72)	0.530	7.09 (6.96)	28
	ITIC-3T	1 : 1	100	0.966	15.77 (15.40)	0.592	9.02 (8.89)	This work
	ITIC-2T	1 : 1	100	0.982	12.28 (11.98)	0.556	6.70 (6.58)	This work
PBDTBDD-Ph	ITIC-4T	1 : 1	—	0.935	16.94 (16.73)	0.625	9.90 (9.82)	This work
	ITIC-3T	1 : 1	—	0.924	17.51 (17.00)	0.681	11.02 (10.86)	This work
	ITIC-2T	1 : 1	—	0.920	13.56 (13.44)	0.502	6.26 (6.18)	This work
PBDTBDD-PhPh	ITIC-4T	1 : 1	—	0.936	16.27 (15.89)	0.513	7.81 (7.65)	This work
	ITIC-3T	1 : 1	—	0.934	15.73 (15.30)	0.523	7.68 (7.49)	This work
	ITIC-2T	1 : 1	—	0.929	12.30 (12.15)	0.461	5.27 (5.11)	This work

[a] The blend films were thermally annealed for 10 min. [b] The calculated J_{SC} from the EQE measurements in brackets. [c] Average PCE in brackets (15 devices).

indicated that the charges transfer effectively before they are recombined, and PSCs with ITIC-3T and ITIC-4T as acceptors have more efficient photo-induced exciton dissociation and charge transport behaviour. The PBDTBDD-Ph/ITIC-2T 珡lm showed the worst PL quenching performance, suggesting that more recombination occurred in the blend 珡lm, leading to poor device performances.

Furthermore, transmission electron microscopy (TEM) was performed to investigate the bulk morphologies of the blend 珡lms. As we reported previously, the blend 珡lm having strong aggregation, *i.e.*, PBDTsTh-BDD and elongated ITIC-4T showed large ball-shaped morphology[28] (Fig. 5a), which decreased exciton migration to the donor/acceptor interface. As shown in Fig. 5b, a泂er blending with small-sized ITIC-3T, the morphology of the blend 珡lms improved. The ball-shaped polymer aggregates signi珡cantly decreased, which resulted in promising PCE. As shown in Fig. 5d, compared with the observation for the PBDTsTh-BDD/ITIC-4T blend 珡lm, the size of ball-shaped polymer aggregates was reduced and PCE of solar cells increased. This can con珡rm our previous viewpoint that weak- ening the aggregations of polymer chains can enhance the photovoltaic property of NF-PSCs. Similarly, a泂er blending with small-sized ITIC-3T (Fig. 5e), the morphology of the blend 珡lms also showed improvement. The number of ball-shaped polymer aggregates reduced signi珡cantly; this was bene珡cial to charge transfer and led to considerable improvement in J_{SC} and FF. Although PCE of 11.02% is relatively satisfactory, some ball- shaped aggregates still existing in the blend limited the photovoltaic performance. The polymer aggregates required further destruction. As shown in Fig. 5g and h, PBDTBDD-PhPh/ITIC-4T and PBDTBDD-PhPh/ITIC-3T blends show much worse morphologies. This could be because the signi珡cantly long biphenyl side chains destroyed the ordered stacking of the polymer PBDTBDD-PhPh and formed large space. As a result, these devices showed very poor PCEs. Thus, it can be found that the polymer needs appropriate aggregation. Other rigid aryl rings (naphthalene and benzothiophene) as side chains may tune aggregation of the polymer well. We will investigate them in a future work. In addition, a泂er decreasing the size of FREA (Fig. 5c, f and i), strong aggregations and severe phase separation occurred in the blends, which were not favorable for charge separation and led to very poor PCEs.

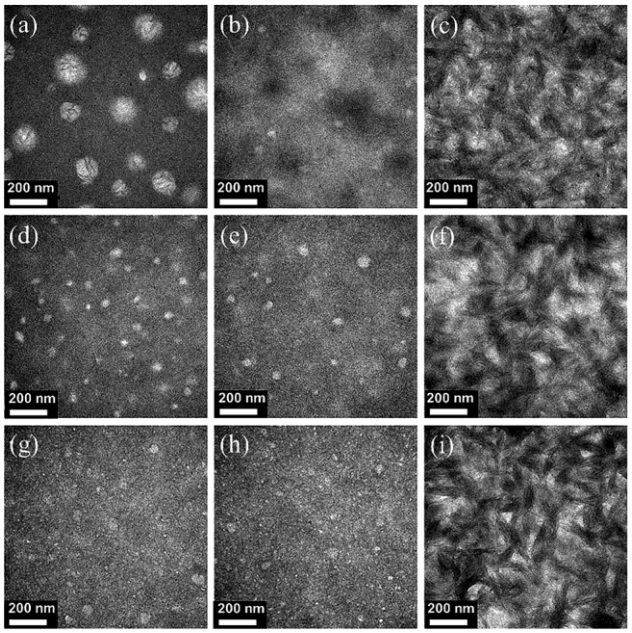

Fig. 5 TEM images of the active layers. (a) PBDTsTh-BDD/ITIC-4T; (b) PBDTsTh-BDD/ITIC-3T; (c) PBDTsTh-BDD/ITIC-2T; (d) PBDTBDD-Ph/ITIC-4T; (e) PBDTBDD-Ph/ITIC-3T; (f) PBDTBDD-Ph/ITIC-2T; (g) PBDTBDD-PhPh/ITIC-4T; (h) PBDTBDD-PhPh/ITIC-3T and (i) PBDTBDD-PhPh/ITIC-2T.

Conclusions

In summary, we designed and synthesized two new wide-bandgap polymers (PBDTBDD-Ph and PBDTBDD-PhPh) with different aggregation degrees and FREAs (ITIC-4T, ITIC-3T and ITIC-2T) with different sizes. The study was used to understand how to design donor polymers and FREAs for high-performance NF-PSCs. The results clearly demonstrated that weakly aggregated donor polymers and small-sized FREAs in appropriate degree could match well with each other to achieve high PCEs. In other words, small-sized FREAs could be embedded more easily into the interspace of polymer chains and weakly aggregated polymers can offer more space for FREAs to intercalate into. Finally, an NF-PSC device based on the weakly aggregated polymer PBDTBDD-Ph and small-sized ITIC-3T yielded over 11% PCE. Thus, this work offers an important guideline for the design of donor polymers and FREAs for high-performance fullerene/fullerene-free PSCs.

Conflicts of interest

There are no con珡icts to declare.

Acknowledgements

This work was supported by the National Natural Science Foundation of China (51573205 and 51773220), China Postdoctoral Science Foundation (2017M612202).

Notes and references

1 J. J. M. Halls, C. A. Walsh, N. C. Greenham, E. A. Marseglia, R. H. Friend, S. C. Moratti and A. B. Holmes, *Nature*, 1995, 376, 498.
2 G. Yu, J. Gao, J. C. Hummelen, F. Wudl and A. J. Heeger, *Science*, 1995, 270, 1789–1791.
3 Y. J. Cheng, S. H. Yang and C. S. Hsu, *Chem. Rev.*, 2009, 109, 5868–5923.
4 A. J. Heeger, *Chem. Soc. Rev.*, 2010, 39, 2354–2371.
5 G. Li, R. Zhu and Y. Yang, *Nat. Photonics*, 2012, 6, 153.
6 Y. Huang, E. J. Kramer, A. J. Heeger and G. C. Bazan, *Chem. Rev.*, 2014, 114, 7006–7043.
7 L. Lu, T. Zheng, Q. Wu, A. M. Schneider, D. Zhao and L. Yu, *Chem. Rev.*, 2015, 115, 12666–12731.

8 C. B. Nielsen, S. Holliday, H.-Y. Chen, S. J. Cryer and I. McCulloch, *Acc. Chem. Res.*, 2015, **48**, 2803–2812.
9 Y. Lin and X. Zhan, *Acc. Chem. Res.*, 2016, **49**, 175–183.
10 Y. Lin, Q. He, F. Zhao, L. Huo, J. Mai, X. Lu, C.-J. Su, T. Li, J. Wang, J. Zhu, Y. Sun, C. Wang and X. Zhan, *J. Am. Chem. Soc.*, 2016, **138**, 2973–2976.
11 Y. Cui, H. Yao, B. Gao, Y. Qin, S. Zhang, B. Yang, C. He, B. Xu and J. Hou, *J. Am. Chem. Soc.*, 2017, **139**, 7302–7309.
12 B. Kan, H. Feng, X. Wan, F. Liu, X. Ke, Y. Wang, Y. Wang, H. Zhang, C. Li, J. Hou and Y. Chen, *J. Am. Chem. Soc.*, 2017, **139**, 4929–4934.
13 H. Bin, Z.-G. Zhang, L. Gao, S. Chen, L. Zhong, L. Xue, C. Yang and Y. Li, *J. Am. Chem. Soc.*, 2016, **138**, 4657–4664.
14 Z. Li, K. Jiang, G. Yang, J. Y. L. Lai, T. Ma, J. Zhao, W. Ma and H. Yan, *Nat. Commun.*, 2016, **7**, 13094.
15 D. Baran, R. S. Ashraf, D. A. Hanifi, M. Abdelsamie, N. Gasparini, J. A. Röhr, S. Holliday, A. Wadsworth, S. Lockett, M. Neophytou, C. J. M. Emmott, J. Nelson, C. J. Brabec, A. Amassian, A. Salleo, T. Kirchartz, J. R. Durrant and I. McCulloch, *Nat. Mater.*, 2016, **16**, 363.
16 Y. Liu, Z. Zhang, S. Feng, M. Li, L. Wu, R. Hou, X. Xu, X. Chen and Z. Bo, *J. Am. Chem. Soc.*, 2017, **139**, 3356–3359.
17 L. Zuo, J. Yu, X. Shi, F. Lin, W. Tang and A. K.-Y. Jen, *Adv. Mater.*, 2017, **29**, 1702547.
18 B. Fan, K. Zhang, X.-F. Jiang, L. Ying, F. Huang and Y. Cao, *Adv. Mater.*, 2017, **29**, 1606396.
19 H. Zhang, H. Yao, J. Hou, J. Zhu, J. Zhang, W. Li, R. Yu, B. Gao, S. Zhang and J. Hou, *Adv. Mater.*, 2018, **30**, 1800613.
20 H. Li, Z. Xiao, L. Ding and J. Wang, *Sci. Bull.*, 2018, **63**, 340–342.
21 Y. Lin, Z.-G. Zhang, H. Bai, J. Wang, Y. Yao, Y. Li, D. Zhu and X. Zhan, *Energy Environ. Sci.*, 2015, **8**, 610–616.
22 Y. Lin, J. Wang, Z.-G. Zhang, H. Bai, Y. Li, D. Zhu and X. Zhan, *Adv. Mater.*, 2015, **27**, 1170–1174.
23 S. Holliday, R. S. Ashraf, A. Wadsworth, D. Baran, S. A. Yousaf, C. B. Nielsen, C.-H. Tan, S. D. Dimitrov, Z. Shang, N. Gasparini, M. Alamoudi, F. Laquai, C. J. Brabec, A. Salleo, J. R. Durrant and I. McCulloch, *Nat. Commun.*, 2016, **7**, 11585.
24 H. Yao, Y. Cui, R. Yu, B. Gao, H. Zhang and J. Hou, *Angew. Chem., Int. Ed.*, 2017, **56**, 3045–3049.
25 W. Wang, C. Yan, T.-K. Lau, J. Wang, K. Liu, Y. Fan, X. Lu and X. Zhan, *Adv. Mater.*, 2017, **29**, 1701308.
26 D. Xie, T. Liu, W. Gao, C. Zhong, L. Huo, Z. Luo, K. Wu, W. Xiong, F. Liu, Y. Sun and C. Yang, *Sol. RRL*, 2017, **1**, 1700044.
27 H. Yao, L. Ye, J. Hou, B. Jang, G. Han, Y. Cui, G. M. Su, C. Wang, B. Gao, R. Yu, H. Zhang, Y. Yi, H. Y. Woo, H. Ade and J. Hou, *Adv. Mater.*, 2017, **29**, 1700254.
28 D. Liu, J. Wang, C. Gu, Y. Li, X. Bao and R. Yang, *Adv. Mater.*, 2018, **30**, 1705870.
29 T. Liu, X. Pan, X. Meng, Y. Liu, D. Wei, W. Ma, L. Huo, X. Sun, T. H. Lee, M. Huang, H. Choi, J. Y. Kim, W. C. H. Choy and Y. Sun, *Adv. Mater.*, 2017, **29**, 1604251.
30 Y. Yang, Z.-G. Zhang, H. Bin, S. Chen, L. Gao, L. Xue, C. Yang and Y. Li, *J. Am. Chem. Soc.*, 2016, **138**, 15011–15018.
31 Y. Firdaus, L. P. Maffei, F. Cruciani, M. A. Müller, S. Liu, S. Lopatin, N. Wehbe, G. O. N. Ndjawa, A. Amassian, F. Laquai and P. M. Beaujuge, *Adv. Energy Mater.*, 2017, **7**, 1700834.
32 D. Liu, K. Zhang, Y. Zhong, C. Gu, Y. Li and R. Yang, *J. Mater. Chem. A*, 2018, **6**, 18125–18132.
33 J. Wang, W. Wang, X. Wang, Y. Wu, Q. Zhang, C. Yan, W. Ma, W. You and X. Zhan, *Adv. Mater.*, 2017, **29**, 1702125.
34 Y. Lin, F. Zhao, Q. He, L. Huo, Y. Wu, T. C. Parker, W. Ma, Y. Sun, C. Wang, D. Zhu, A. J. Heeger, S. R. Marder and X. Zhan, *J. Am. Chem. Soc.*, 2016, **138**, 4955–4961.
35 Y. Lin, T. Li, F. Zhao, L. Han, Z. Wang, Y. Wu, Q. He, J. Wang, L. Huo, Y. Sun, C. Wang, W. Ma and X. Zhan, *Adv. Energy Mater.*, 2016, **6**, 1600854.
36 C. Lee, W. Yang and R. G. Parr, *Phys. Rev. B: Condens. Matter Mater. Phys.*, 1988, **37**, 785–789.
37 C. M. Cardona, W. Li, A. E. Kaifer, D. Stockdale and G. C. Bazan, *Adv. Mater.*, 2011, **23**, 2367–2371.
38 Y. Shen, A. R. Hosseini, M. H. Wong and G. G. Malliaras, *ChemPhysChem*, 2004, **5**, 16–25.